Journal of Materials Chemistry C

Accepted Manuscript

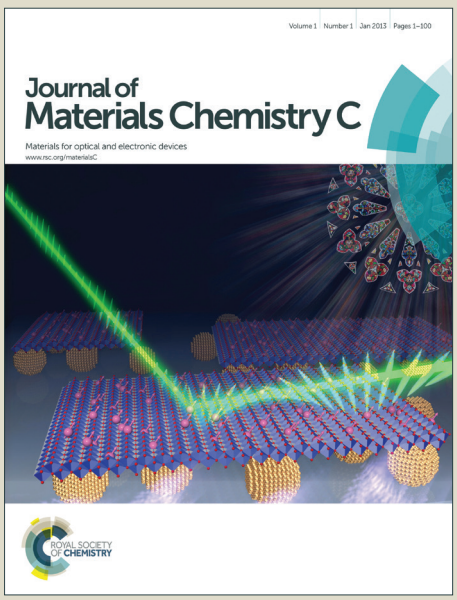

ROYAL SOCIETY OF CHEMISTRY

www.rsc.org/materialsC

Journal of Materials Chemistry C

ARTICLE

Dual emissive analogue of deoxyuridine as a sensitive hydration-reporting probe for discriminating mismatched from matched DNAs and DNA/DNA and DNA/RNA duplexes

Received15th October 2015,
Accepted 00th January 20xx

DOI: 10.1039/x0xx00000x

www.rsc.org/

Nicolas P. F. Barthes,[a‡] Krishna Gavvala,[b‡] Dmytro Dziuba,[a,] Dominique Bonhomme,[a] Iuliia A. Karpenko,[a,] Anne S. Dabert-Gay,[c] Delphine Debayle,[c] Alexander P. Demchenko,[d] Rachid Benhida,[a] Benoît Y. Michel,[a] Yves Mély,[*b] and Alain Burger[*a]

Fluorescent nucleosides with high sensitivity to H-bonding are of great interest not only to investigate DNA hydration and DNA-protein interactions and dynamics, but also to develop screening assays. Here, we report on the incorporation of a dual emissive uridine analogue based on the 3-hydroxychromone scaffold (3HC) into DNA oligonucleotides of different sequences and the characterization of the spectroscopic properties of the labelled oligonucleotides in matched and mismatched duplexes and in duplexes of different forms. The probe exhibits two-colour emission and spectral λ-shift, which vary as a function of the local hydration of the 3HC. It provides the highest sensitivity together with calibration on the molecular level, which allow discriminating between matched and mismatched dsDNA, as well as between B- and A-forms of DNA/DNA and DNA/RNA duplexes. We suggest that the physical basis of such reporting is the change of hydration in close proximity of the fluorescent base emitter which appears ideally suitable for such sensing.

Introduction

Novel fluorescent derivatives of DNA bases that report high sensitivity on hydration are of great interest for investigating DNA hydration and folding, DNA-protein interactions and dynamics, as well as for developing screening assays. They are expected to emerge as new sensitive tools since water-coating of DNAs plays a key role in determining their folding, conformations and interactions. Indeed, water molecules bound to DNA display hydration patterns and physical properties that are different from bulk water and specific to each DNA form.[1-12] On the other hand, the binding of proteins or drugs to nucleic acids is also well known to impact the water distribution in contact with DNA.[4,13-15]

Environment-sensitive fluorophores exhibiting solvatochromic properties are important tools for fluorescence molecular sensing. Steady-state and time-resolved fluorescence spectra of solvatochromic dyes contain in particular the information about specific and non-specific interactions of the probe with the surrounding molecules and the rates of the media relaxation. Different solvatochromic dyes were investigated to interrogate the polarity of the minor and major grooves and different conformations of the DNA by monitoring the changes in the absorption and/or emission maxima.[16-26] The dielectric constant and Lippert-Mataga scales[27,28] were employed to estimate the polarity of the local environment of the probes. However, exploiting these scales to estimate the polarity in hydrated media is not fully satisfactory since they do not take into account the contribution of specific H-bonding interactions.[17] Such interactions are particularly critical for probes having a conjugated donor–acceptor system (e.g. dansyl fluorophores: DAN),[17,20,29] being in contact to water in the considered grooves. The usage of the Reichardt scale[30] gives in general better correlations because this empirical scale accounts for the dielectric constant of the solvent and its H-bond donor ability. As a consequence, the introduction of a fluorescent probe to sense the DNA grooves and displaying high sensitivity to H-bonding rather than to dipolar interactions was hitherto lacking.[17]

An ideal hydration-sensitive probe should satisfy several additional demands. It should be incorporated in a way that does not perturb the nucleic acid structure being located either in the major or minor groove of dsDNA. The H-bond sensor (usually an oxygen of a carbonyl, amide or sulfonamide

[a] Institut de Chimie de Nice, UMR 7272, Université de Nice Sophia Antipolis, CNRS, Parc Valrose, 06108 Nice Cedex 2, France.
[b] Laboratoire de Biophotonique et Pharmacologie, UMR 7213, Faculté de Pharmacie, Université de Strasbourg, CNRS, 74 Route du Rhin, 67401 Illkirch, France.
[c] Institut de Pharmacologie Moléculaire et Cellulaire, UMR 6097, Université de Nice Sophia Antipolis, 660 Route des Lucioles, 06560 Valbonne, France
[d] A.V. Palladin Institute of Biochemistry, 9 Leontovicha Street, Kiev 01030, Ukraine.
* burger@unice.fr, yves.mely@unistra.fr
‡These authors contributed equally. These authors contributed equally
Electronic Supplementary Information (ESI) available: [details of any supplementary information available should be included here]. See DOI: 10.1039/x0xx00000x

group)[17,20,29] should be located in a position that is sensitive to DNA transformations by shifting between H-bond free and H-bonded forms. To address all these requirements, we have recently reported a new dual emissive nucleoside **1** (Figure 1) highly sensitive to hydration.[31,32] The new probe was engineered by connecting the 2-thienyl-3-hydroxychromone (3HC) fluorophore to the 5-position of deoxyuridine via an ethynyl bond to favour interactions with water molecules rather than to substitute a natural base by the dye.[33,34] A rigid acetylenic linker was chosen to locate the dye in a precise position with respect to the DNA major axis with the aim to restrain undesired contact with H-bond donor and acceptor groups of DNA. Such control is of key importance for further data interpretation of hydration and biomolecular interaction studies.

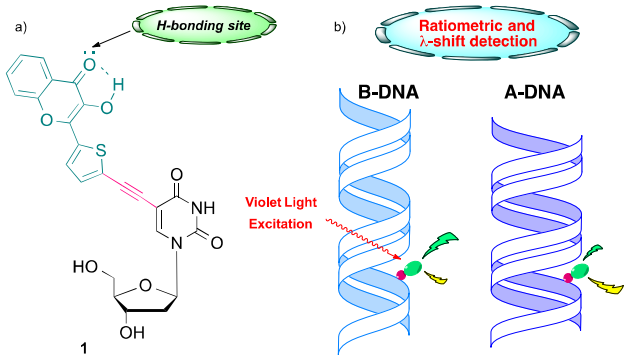

Figure 1. a) Structure of the dual emissive deoxyuridine conjugate **1** and b) Representative concept for the conformational study of hybrid duplexes based on the ratiometric detection of the local hydration changes.

Due to an excited state intramolecular proton transfer reaction (ESIPT),[35] **1** can exist in two excited states, the normal (N*) and the tautomer (T*) forms, that emit light with different energies and provide two well-separated emission bands (Scheme 1).

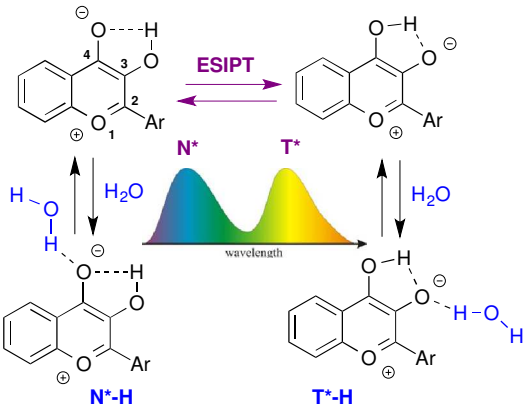

Scheme 1. Proposed mechanism for water sensing by 3HC **1** adapted from.[31] Excited states N* and N*-H, and T* and T*-H of the normal and tautomer forms are in equilibrium.[36] N*-H undergoes ESIPT reaction in a much slower time scale than N*. N* and N*-H, and T* and T*-H generate the higher and lower energy emission bands, respectively referred as N* and T* on the spectrum for simplification.

In the excited normal state (N*), the oxygen carbonyl at 4-position of 3HC becomes more basic, making this group subject to formation of H-bonds with protic solvents. In particular, **1** demonstrates high sensitivity to hydration since an increase in water concentration inhibits the ESIPT reaction and thus, increases the relative intensity of the N* band (Figure 2).[31] Moreover, hydration also favours H-bonding of the tautomer forms, which results in the blue-shift of the T* emission maximum as a consequence of the more stabilized ground state and the increased energy gap between the excited and ground states of the hydrated forms.[37] Therefore, measuring the intensity ratios of the two emission bands (I_{N*}/I_{T*}) and also the λ-shifts of the T* band allows monitoring, by two different channels of information, the hydration changes in the vicinity of the 3HC. Additionally, the newly synthesized dye absorbs strongly in the violet (λ_{Abs} ~ 400 nm), exhibits large Stokes shifts (> 100 nm), keeps significant quantum yield in water (6%), which is unusual among polarity-sensitive dyes, and thus possesses useful properties for selective excitation and easier detection.[38-41]

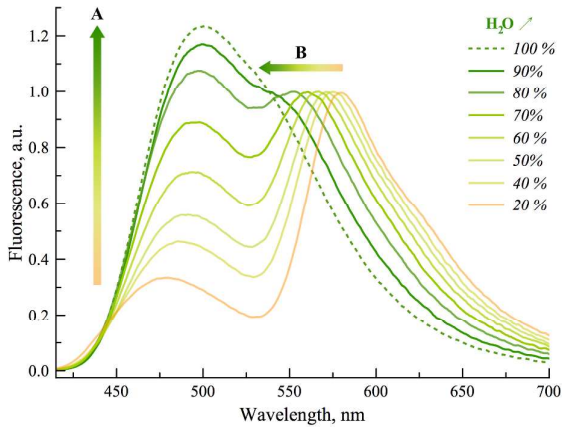

Figure 2. Two-band ratiometric and wavelength-shifting responses of conjugate **1** to hydration in water-dioxane mixtures..[31] Growing water concentration results in the relative increase of the N* band and the blue-shift of the maximum of the T* band emission: A and B arrows, respectively. The fluorescence spectra are normalized by T* band.

Successful synthesis of the conjugate **1** with such remarkable spectroscopic properties stimulated our efforts to obtain oligodeoxynucleotides (ODNs) with its incorporation. In this work, we describe the synthesis and photophysical properties of such labelled ODNs. We demonstrate that the incorporated nucleoside is able to probe the hydration of the major groove and to discriminate the environmental and conformational changes of DNA/DNA and DNA/RNA duplexes of different compositions (Figure 1b).

Journal of Materials Chemistry C

ARTICLE

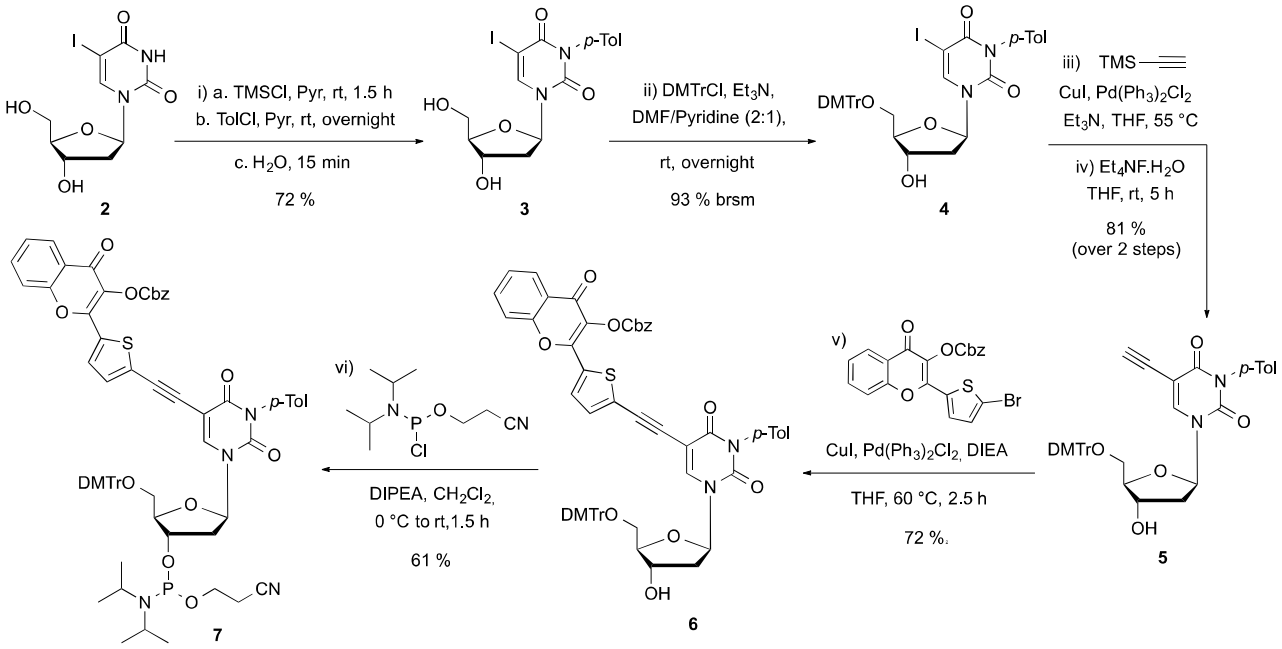

Scheme 2. Synthesis of the phosphoramidite of the conjugate 3HC-deoxyuridine **1**.

RESULTS AND DISCUSSIONS

Synthesis and photophysical properties of labelled DNA and DNA/DNA duplexes

The synthesis of the phosphoramidite **7** required for the preparation of the labelled ODNs is described in Scheme 2. The synthetic approach was adapted from the procedure developed for dye **1**.[31] The protection of the 3-imido and 5'-hydroxyl groups of **2**, provided the 5-iododeoxyuridine derivative **4**. This intermediate was then engaged in a first Sonogashira coupling with trimethylsilylacetylene. Subsequent treatment with tetraethylammonium fluoride gave the terminal alkyne **5**. Concerning the final assembly, a second Sonogashira coupling with the bromothienyl chromone partner afforded the conjugate **6** of 3HC and deoxyuridine. Phosphitylation of **6** under classical conditions yielded phosphoramidite **7**, which was used for the solid-phase synthesis of the labelled 15-mer ODNs (SI). HPLC, UV and MS analysis ascertained the purity and integrity of the synthesized ODNs (Table S1, Figures S1, S2, S3 & S4).

The 15-mer d(CGT TTT **XMX** TTT TGC) sequences, where **X** = **T**, **A**, **C** and **G** and **M** = conjugate **1**, were chosen as model sequences to characterize the photophysical properties of **1** in different ODN contexts. The conjugate was positioned in the middle rather than at a terminal position of the duplexes in order to avoid structural disorders due to end effects. The sequences referred as **TMT, AMA**, **CMC** and **GMG** differed by the residues flanking the modified nucleotide **1**. Control experiments were performed with wild-type strands of composition d(CGT TTT **XTX** TTT TGC). Each ODN was then annealed with its complementary ODN (noted in italic) containing a natural base or an abasic site at the position opposite **1**, resulting in duplexes of different compositions (Table 1 and SI). The sequences of the complementary strands were *d(GCA AAA **YXY** AAA ACG)*, where ***Y*** = ***A***, ***T***, ***C*** or ***G*** and ***X*** is any of the natural bases (matched and mismatched pairs) or an abasic site (***Ab***). We first assessed whether the deoxyuridine derivative **1** selectivity base pairs with **A** and does not affect the secondary structure of the duplexes by monitoring the temperature-induced absorbance changes at 260 nm and recording the CD spectra (Tables 1 & S2, Figures S5, S6 & S7).

Thermal denaturation studies showed that the most stable labelled duplexes were obtained with the fully complementary sequences. The labelled duplexes were slightly less stable than the corresponding wild-type matched and mismatched duplexes (ΔT_m = -1 to -4.9 °C) except for ***C*** opposite **1** (ΔT_m = 0.1 to 3.6 °C, Tables 1 & S2). Comparable observations were reported for other hydrophobic moieties, such as phenanthroline, anthracene, and pyrene, connected to ***U*** via an acetylenic linker.[42-44] Remarkably, labelled duplexes containing an abasic site were significantly more stable than the corresponding controls (ΔT_m = +4.7 to +7 °C). The increase of T_m of the **M-*Ab*** duplexes suggests that the dye accommodates well the abasic lesion and stabilizes the duplex, likely through its large stacking area and hydrophobic character.[45] Furthermore, analysis of the CD spectra showed that the label did not affect the B-helix conformation of the DNA/DNA duplexes (Figures 3 & S7).

In a next step, the UV absorbance and fluorescence spectra of **1** in the single and double stranded forms were recorded in phosphate buffer pH 7.0 (Figures 4, S8, S9, S10, S11 & S12). The spectroscopic characteristics of the labelled sequences together with the data of the monomer **1** in water-dioxane mixtures are reported in Table 1.

The fully complementary dsODNs showed absorption bands centred at 394 and 400 nm while the absorption maxima of the single strands and mismatched duplexes were in the range of 404-409 nm. The positions of the absorption maxima in the fully complementary dsODNs are close to the absorption maximum of the monomer **1** in water-dioxane mixtures suggesting that the dye is more accessible to water than in the single strands and mismatched duplexes. By contrast to matched duplexes, the bathochromic shift of about 7-11 nm observed for the single strands and mismatched duplexes (Figure S8 and Table 1) suggests π- π interactions of the hydrophobic dye with the surrounding bases. Similar effects were reported for the pyrenecarboxamide chromophore anchored at the surface of the major groove of DNA.[26] A red-shift of the absorption maximum is also commonly observed with intercalating dyes. The dye in duplexes with an abasic site exhibited the largest red-shift, confirming its suitable intercalation in these sequences.

The fluorescence spectra showed two well-resolved bands of emission (Figures 4, S9, S10, S11 & S12). Comparison of the spectra revealed that the matched duplexes displayed the highest I_{N*}/I_{T*} ratio and the more blue-shifted T* band (Table 1, Figures 4, S9, S10, S11 & S12). For instance, for the matched **TMT-*AAA*** duplex, the intensity ratio I_{N*}/I_{T*} and emission maximum of the T* band were 1.21 and 548 nm, respectively; while for the **TMT** single strand and the mismatched duplexes, they were in the 0.4-0.63 and 572-573 nm ranges, respectively.

Table 1. Spectroscopic data for conjugate **1** and labelled ODNs.

Samples[a,b]	T_m (°C)[c]	% H_2O[a]	λ_{abs} (nm)[d]	λ_{N*} (nm)[e]	λ_{T*} (nm)[f]	I_{N*}/I_{T*}[g]	Φ (%)[h]
1		100	395	500[i]	-		6
		90	394	497	539	1.17	6
		80	395	498	552	1.08	8
		70	395	494	561	0.89	26
		60	395	493	567	0.72	27
		50	394	490	571	0.56	25
TMT	-		405	493	572	0.63	13
TMT·*AAA*	45.8		397	487	548	1.21	11
TMT·*ATA*	37.9		404	491	573	0.53	12
TMT·*ACA*	39.1		405	491	573	0.40	16
TMT·*AGA*	38.1		406	490	573	0.57	6
TMT·*AAbA*	39.2		408	492	573	0.47	11
TMT·*rAAA*	40.6		399	483	561	0.90	19
TMT·r_M*AAA*	38.8		402	487	566	0.78	20
TMT·r_M*AUA*	29.2		406	492	569	0.68	33
AMA	-		407	492	570	0.63	9
AMA·*TAT*	42.4		400	488	552	1.21	8
AMA·*TTT*	37.6		406	495	571	0.48	11
AMA·*TCT*	39.2		407	493	574	0.47	11
AMA·*TGT*	38.1		407	491	571	0.58	9
AMA·*TAbT*	36.3		408	497	573	0.67	13
AMA·r_M*UAU*	37.1		406	490	564	0.85	15
CMC	-		405	493	569	0.70	9
CMC·*GAG*	48.1		394	487	548	1.00	9
CMC·*GTG*	37.9		407	489	565	0.92	4
CMC·*GCG*	42.6		412	492	569	0.83	3
CMC·*GGG*	42.5		406	490	567	0.76	4
CMC·*GAbG*	43.2		409	493	570	0.84	3
GMG	-		408	491	573	0.66	3
GMG·*CAC*	52.4		400	488	561	1.00	1
GMG·*CTC*	45.6		407	490	572	0.60	2
GMG·*CCC*	47.1		406	489	569	0.43	2
GMG·*CGC*	47.3		407	488	571	0.84	1
GMG·*CAbC*	44.5		409	490	573	0.60	2

a) 2 µM of monomer **1** in water-dioxane mixtures; b) 2 µM of ODN in buffer pH 7.0 (20 mM Sodium phosphate, 150 mM NaCl, 1 mM EDTA); c) Melting temperature; ±0.5°C; d) Position of the absorption maximum; e) Position of the emission maximum of the normal N* band; f) Position of the emission maximum of the tautomer T* band; g) I_{N*}/I_{T*} corresponds to the ratio of the intensities of the two emission bands at their maxima; ±2.5% mean standard deviation; h) Quantum yields determined using quinine sulfate (QS) in 0.1 M HCl solution (λ_{ex} = 350 nm, Φ= 0.54)[46] and *p*-dimethylaminoflavone (dMAF) in EtOH (λ_{ex} = 404 nm, Φ= 0.27)[47] as references, ±10% mean standard deviation; i) In water, the N* and T* bands collapse in a single band.

The intensity ratios and the maxima of the T* emission of the matched duplexes were close to the values obtained for **1** in 90 % water, while the corresponding values in the single strands and mismatched duplexes were close to the values observed for **1** in 50 % water (Table 1, Figures 2 and 4). Noticeably, **TMT** and **AMA** single and double strands gave very close results, indicating that the spectroscopic properties of conjugate **1** are similarly influenced by **T** and **A** flanking bases (Table 1, Figures 4, S8, S9 & S10).

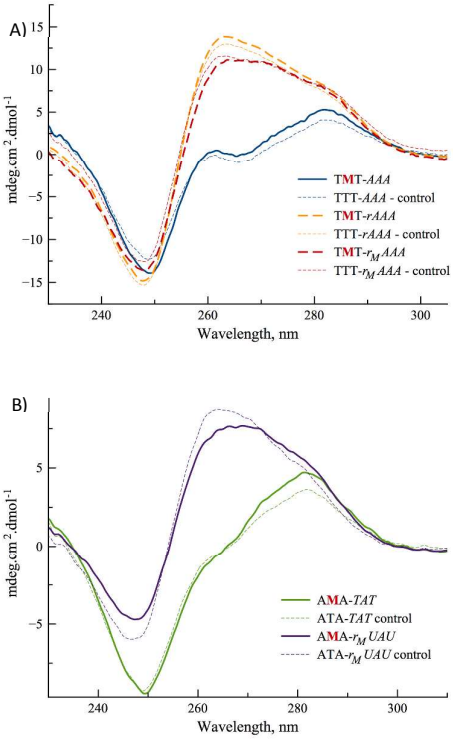

Figure 3. CD spectra of matched (A) **TMT-*AAA***, **TMT-r_M*AAA***, **TMT-*rAAA*** (B) **AMA-*TAT***, **AMA-r_M*UAU*** and their native wild type duplexes recorded in pH 7.0 buffer (20 mM Sodium phosphate, 150 mM NaCl, 1 mM EDTA).

The **CMC** and **GMG** sequences followed similar trend (Figures S11 & S12). Nevertheless, the intensity ratios of the fully matched duplexes were smaller than those obtained for the corresponding **TMT** and **AMA** double strands indicating than the dye is exposed in a slightly less hydrated environment (compare 1 with 1.21, similar to the values obtained for **1** in about 80 % water). All the **TMT** and **AMA** ODNs, and the **CMC** single and matched double strands gave similar or larger quantum yields as compared to that of the free dye **1** in water. The fluorescence quantum yield of the dye in these single- and double-stranded ODNs varied from 6 to 16 %. By contrast the mismatched duplexes of **CMC** and all the **GMG** ODNs gave lower quantum yields suggesting a direct contact quenching of **1** by ***G*** in these ODNs. Quenching of fluorescent nucleoside analogues in ODNs by ***G*** is common.[48,49]

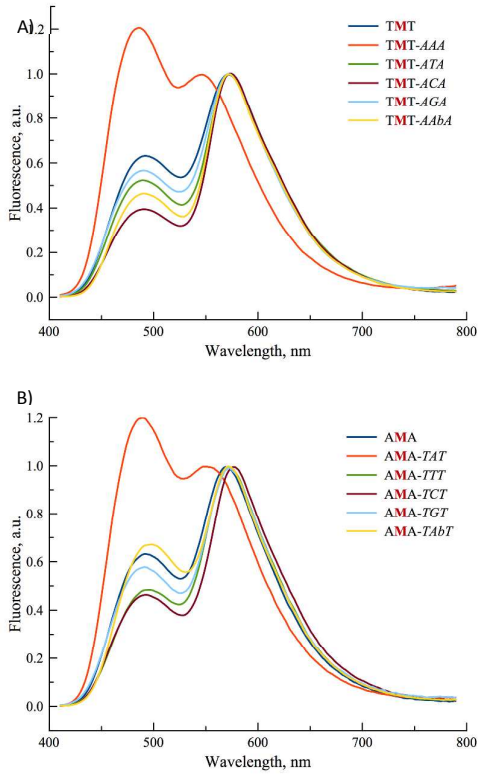

Figure 4. Fluorescence spectra of ss, matched (A) **TMT** & **TMT-*AXA***, (B) **AMA, AMA-*TXT*** and their corresponding mismatched duplexes recorded in pH 7.0 buffer (20 mM Sodium phosphate, 150 mM NaCl, 1 mM EDTA) and normalized by T* band.

Taken together, our data indicate that the analysis of the two channels of information of the label allows easily distinguishing the matched duplexes from the single strands and mismatched duplexes. The ODNs with **A** and **T** flanking the label demonstrate the highest sensitivity for discriminating matched from mismatched bases. The I_{N*}/I_{T*} channel demonstrates superior sensitivity, up to 40 fold, to distinguish matched from mismatched duplexes with variation in I_{N*}/I_{T*} from 10 to 200 %[§] as compared to the 5 % variation of the shift of the T* band. Since H-bonding and hydration are driving the response of the two channels of information,[31] our data strongly suggest that in matched duplexes the label is exposed to a more hydrated environment as compared to the single strands and mismatched duplexes. For the latter, probe **1** is partially shielded from the water due to the accommodation of the dye with its surrounding nucleobases through favourable hydrophobic and stacking interactions of the thienyl-chromone conjugate (Figure 5). This interpretation is supported by the fact that the mismatched duplexes exhibit higher melting temperatures than the corresponding wild type mismatched dsDNA and red-shifted absorption maxima compared to the perfectly matched labelled dsDNA. The 2-3 fold reduced quantum yields of the mismatched dsDNA of **CMC** relative to that of the matched duplex provide further evidence of direct contact with the

surrounding nucleobases (*vide supra*). Noticeably, the label is able to sense in the fully matched DNA the subtle change in hydration of the local environment of **G/C** and **A/T** base pairs.[2] It distinguishes remarkably from the DAN (6-dimethylamino-2-acylnaphthalene) fluorophore, which was unable to detect such changes.[24]

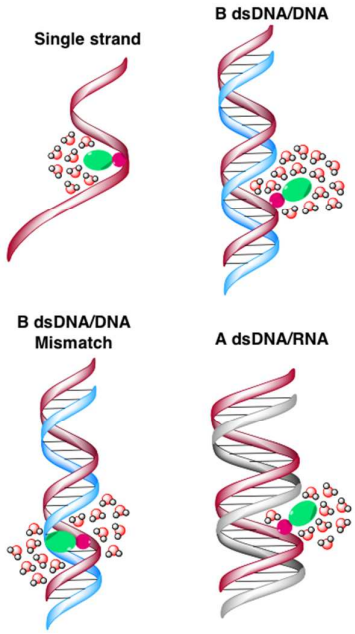

Figure 5. Schematic representation of the different hydrated environments of probe **1** in single strand, matched and mismatched DNA/DNA duplexes, and DNA/RNA hybrid.

Discrimination of DNA/DNA and DNA/RNA duplexes

Next, we examined the ability of **1** to monitor the transition from B- to A-form duplexes at constant ionic strength.[§§] Such transition is physiologically important as it is produced for instance in base pairing of DNA and RNA strands during transcription and it is thought to govern a number of protein/DNA interactions.[6,50]

The **TMT** and **AMA** sequences were selected as representative pyrimidine and purine flanking bases, respectively. For convenience, the more stable methoxy RNA was used for hybridization with DNA because the modification of the minor groove with the 2'-OMe group is known to keep the A conformation unaffected.[51] Thus, **TMT** and **AMA** were annealed with the complementary 2'-OMe RNA strands r_M*(GCA AAA YAY AAA ACG)*, where ***Y*** is ***A*** or ***U***, and referred as $\boldsymbol{r_MAAA}$ and $\boldsymbol{r_MUAU}$, respectively. Control experiments were conducted with **TMT** annealed with the 2'-OH RNA strand ***rAAA*** and the single mismatched 2'-OMe RNA strand $\boldsymbol{r_MAUA}$ corresponding to *r(GCA AAA AAA AAA ACG) and* r_M*(GCA AAA AUA AAA ACG), respectively*. Upon hybridization of RNA to DNA, a clear difference in the secondary structure of the obtained hybrids in comparison to the DNA/DNA duplexes was evidenced from the CD spectra (Figure 3). A characteristic blue-shift of the positive band, as well as an increase in its amplitude were observed, as expected.[52] The impact of probe **1** on the stability of the hybrids was comparable to that observed for DNA/DNA duplexes (Table S2).

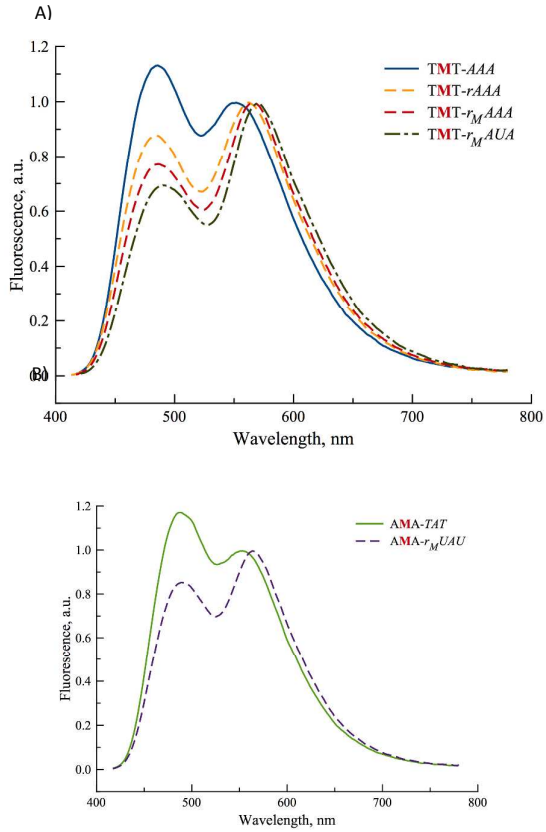

Figure 6. Fluorescence spectra of (A) **TMT-*AAA*, TMT-r_M*AAA*** and **TMT-*rAAA*, TMT-r_M*AUA*** (B) **AMA-*TAT*** and **AMA-*rUAU*** recorded in pH 7.0 buffer (20 mM Sodium phosphate, 150 mM NaCl, 1 mM EDTA) and normalized by T* band.

The absorption and fluorescence characteristics of the different hybrids are given in Table 1. The fluorescence spectra of the matched methoxy DNA/RNA duplexes revealed dramatic changes relative to the B-form duplexes (Figures 6). For instance in the case of **TMT-$\boldsymbol{r_M}$*AAA***, the intensity ratio I_{N*}/I_{T*} and emission maximum of the T* band were 0.78 and 566 nm, respectively. Importantly, the **TMT-*rAAA*** duplex showed similar trends, also the decrease of the intensity ratio I_{N*}/I_{T*} and red shift of the T* band were less pronounced. Comparison of the values of the 2'-OMe and 2'-OH duplexes with that of **TMT-*AAA*** gave a 1.6 and 1.3 fold ratio decrease, and 16 and 13 nm red-shift, respectively. As expected, the control experiment conducted with the mismatched **TMT-$\boldsymbol{r_M}$*UAU*** furnished the more pronounced decrease of the intensity ratio and bathochromic shift of the T* band as observed previously for mismatched dsDNA.

It is noteworthy that the I_{N*}/I_{T*} values of **TMT-$\boldsymbol{r_M}$*AAA*** and **TMT-*rAAA*** were comparable to the values obtained for

dye **1** in 60 and 70% water, respectively (Table 1), indicating that the local environment of the dye was less hydrated in the DNA/RNA hybrid than in the DNA/DNA duplex. Hence, all the combined data are consistent with the lower hydration of the narrower and deeper major groove of A-DNA in comparison to the one of B-DNA.[24,53,54] These results further illustrate that the proper positioning of the water-sensitive reporting carbonyl group of **1** affords a highly sensitive and straightforward method to discriminate B from A duplexes. Compared to the DAN fluorophore classically used for the same purpose,[24] probe **1** demonstrates an about 11 fold-enhanced sensitivity to detect such transition with a 55 % variation in I_{N*}/I_{T*} for **1** as compared to 5% variation of the λ-shift of the emission maximum for DAN. It is also important to note that **1** was able to discern the 2'-OMe and 2'-OH duplexes. Although the 2'-OMe modification is on the minor groove side, it should not affect the shape of the deeper groove. Therefore, the observed difference of the fluorescence signal might rather reflect the change of hydration in the major groove in line with the results of computational simulation that showed that the 2'-OMe modification impacts the distribution of the water molecules.[51]

Conclusions

In this report, ODNs labelled with a new fluorescent conjugate of 3HC and deoxyuridine were synthesized and characterized. It was shown that the unique property of the designed 3HC derivative to provide high sensitive wavelength-ratiometric response to H-bonding is retained on its incorporation into oligonucleotides of different sequences. Monitoring the two channels of information (I_{N*}/I_{T*} ratio and λ-shift of T*) allows estimating the local hydration and discriminating matched from mismatched DNA/DNA duplexes. Moreover, this conjugate enables also to detect the difference between the B and A forms of DNA/DNA and DNA/RNA duplexes, respectively, demonstrating ~ 10-fold increased sensitivity over the DAN fluorophore.[24] The high sensitivity to hydration displayed in two information channels[55] is also reflected in the capacity of the probe to sense subtle changes in hydration of the local environment of **G/C** and **A/T** base pairs in perfectly matched DNA/DNA duplexes and of the major groove in 2'-OMe and wild type DNA/RNA hybrids. The usage of the new fluorophore should open the access to a variety of applications in DNA research that includes site-specific monitoring of local DNA hydration, DNA folding and conformational changes, protein-DNA interactions and dynamics, to name a few. The studies of excision of damaged bases by enzymes involved in the DNA repair machinery are the focus of our current research. They will be reported elsewhere in a close future.

Acknowledgements

We thank the ANR (ANR-12-BS08-0003-02), PACA région (DNAfix-2014-02862 and 2014-07199) and the FRM (DCM20111223038) for financial support and a grant for N.P.F.B. We thank the French Government for the Master 2 grant to I.A.K. and Campus France for the Raman-Charpak fellowship to K.G.

Notes and references

§ Calculated by comparison with the largest and smallest intensity ratios of the mismatched duplexes, respectively.
§§ The effect of the ionic strength on the conformation of the duplex and fluorescence properties of the probe was investigated with **TMT-*AAA*** at different concentrations of NaCl (from 150 mM to 1.5 M). Increasing the ionic strength up to 1.5 M did not promote the transition from B to A conformation in agreement with the fact that A/T rich DNA sequences are resistant to such transition at high ionic strength.[54] No change of the intensity ratio (Figures S14) was also noticed indicating that hydration of the microenvironment of dye **1** of this this B DNA duplex was unaffected and that dye **1** was insensitive to the effect of ionic strength at the tested concentrations of NaCl.

1 P. Auffinger and E. Westhof, *Curr. Opin. Struct. Biol.*, 1998, **8**, 227–236.
2 M. Feig and B. M. Pettitt, *Biopolymers*, 1998, **48**, 199–209.
3 V. Makarov, B. M. Pettitt and M. Feig, *Acc. Chem. Res.*, 2002, **35**, 376–384.
4 B. Jayaram and T. Jain, *Annu. Rev. Biophys. Biomol. Struct.*, 2004, **33**, 343–361.
5 D. Miyoshi, H. Karimata and N. Sugimoto, *J. Am. Chem. Soc.*, 2006, **128**, 7957–7963.
6 I. Brovchenko, A. Krukau, A. Oleinikova and A. K. Mazur, *J. Am. Chem. Soc.*, 2008, **130**, 121–131.
7 S.-I. Nakano, D. Yamaguchi, H. Tateishi-Karimata, D. Miyoshi and N. Sugimoto, *Biophys. J.*, 2012, **102**, 2808–2817.
8 P. Ball, *Chem. Rev.*, 2008, **108**, 74–108.
9 J. Choi and T. Majima, *Chem. Soc. Rev.*, 2011, **40**, 5893–5909.
10 I. Son, Y. L. Shek, D. N. Dubins and T. V. Chalikian, *J. Am. Chem. Soc.*, 2014, **136**, 4040–4047.
11 T. Zubatiuk, O. Shishkin, L. Gorb, D. Hovorun and J. Leszczynski, *J. Phys. Chem. B*, 2015, **119**, 381–391.
12 K. E. Furse and S. A. Corcelli, *J. Phys. Chem. Lett.*, 2010, **1**, 1813–1820.
13 C. K. Reddy, A. Das and B. Jayaram, *J. Mol. Biol.*, 2001, **314**, 619–632.
14 P. L. Privalov, A. I. Dragan, C. Crane-Robinson, K. J. Breslauer, D. P. Remeta and C. A. S. A. Minetti, *J. Mol. Biol.*, 2007, **365**, 1–9.
15 S.-I. Nakano, D. Miyoshi and N. Sugimoto, *Chem. Rev.*, 2014, **114**, 2733–2758.
16 R. W. Sinkeldam, N. J. Greco and Y. Tor, *ChemBioChem*, 2008, **9**, 706–709.
17 R. W. Sinkeldam and Y. Tor, *Org. Biomol. Chem.*, 2007, **5**, 2523.
18 V. R. Jadhav, D. A. Barawkar and K. N. Ganesh, *J. Phys. Chem. B*, 1999, **103**, 7383–7385.

19 A. Okamoto, K. Tainaka and Y. Fujiwara, *J. Org. Chem.*, 2006, **71**, 3592–3598.
20 K. Tainaka, K. Tanaka, S. Ikeda, K.-I. Nishiza, T. Unzai, Y. Fujiwara, I. Saito and A. Okamoto, *J. Am. Chem. Soc.*, 2007, **129**, 4776–4784.
21 R. Jin and K. J. Breslauer, *Proc. Natl. Acad. Sci. U.S.A.*, 1988, **85**, 8939–8942.
22 G.-Q. Tang, N. Tanaka and S. Kunugi, *Bull. Chem. Soc. Jpn.*, 1999, **72**, 1129–1137.
23 T. Kimura, K. Kawai and T. Majima, *Chem. Commun.*, 2006, 1542.
24 T. Kimura, K. Kawai and T. Majima, *Org. Lett.*, 2005, **7**, 5829–5832.
25 A. Okamoto, K. Tainaka and I. Saito, *Bioconjugate Chem.*, 2005, **16**, 1105–1111.
26 A. Okamoto, K. Kanatani and I. Saito, *J. Am. Chem. Soc.*, 2004, **126**, 4820–4827.
27 E. Z. Lippert, *Z. Naturforsch. A*, 1955, 541–545.
28 N. Mataga, Y. Kaifu and M. Koizumi, *Bull. Chem. Soc. Jpn*, 1956, **29**, 465–470.
29 J. R. Lakowicz, *Principles of Fluorescence Spectroscopy*, 3rd edn. 2006.
30 C. Reichardt, *Chem. Rev.*, 1994, **94**, 2319–2358.
31 N. P. F. Barthes, I. A. Karpenko, D. Dziuba, M. Spadafora, J. Auffret, A. P. Demchenko, Y. Mely, R. Benhida, B. Y. Michel and A. Burger, *RSC Adv.*, 2015, **5**, 33536–33545.
32 D. Dziuba, I. A. Karpenko, N. P. F. Barthes, B. Y. Michel, A. S. Klymchenko, R. Benhida, A. P. Demchenko, Y. Mely and A. Burger, *Chem. Eur. J.*, 2014, **20**, 1998–2009.
33 M. Spadafora, V. Y. Postupalenko, V. V. Shvadchak, A. S. Klymchenko, Y. Mely, A. Burger and R. Benhida, *Tetrahedron*, 2009, **65**, 7809–7816.
34 D. Dziuba, V. Y. Postupalenko, M. Spadafora, A. S. Klymchenko, V. Guérineau, Y. Mely, R. Benhida and A. Burger, *J. Am. Chem. Soc.*, 2012, **134**, 10209–10213.
35 A. P. Demchenko, K.-C. Tang, K. C. Tang and P.-T. Chou, *Chem. Soc. Rev.*, 2013, **42**, 1379–1408.
36 V. V. Shynkar, A. S. Klymchenko, E. Piémont, A. P. Demchenko and Y. Mely, *J. Phys. Chem. A*, 2004, **108**, 8151–8159.
37 C. A. Kenfack, A. S. Klymchenko, G. Duportail, A. Burger and Y. Mely, *Phys. Chem. Chem. Phys.*, 2012, **14**, 8910–8918.
38 Y. Niko, Y. Cho, S. Kawauchi and G.-I. Konishi, *RSC Adv.*, 2014, **4**, 36480–36484.
39 A. S. Klymchenko and A. P. Demchenko, *New J. Chem.*, 2004, **28**, 687.
40 O. M. Zamotaiev, V. Y. Postupalenko, V. V. Shvadchak, V. G. Pivovarenko, A. S. Klymchenko and Y. Mely, *Bioconjugate Chem.*, 2011, **22**, 101–107.
41 P. A. Hopkins, R. W. Sinkeldam and Y. Tor, *Org. Lett.*, 2014, **16**, 5290–5293.
42 D. J. Hurley, S. E. Seaman, J. C. Mazura and Y. Tor, *Org. Lett.*, 2002, **4**, 2305–2308.
43 Q. Xiao, R. T. Ranasinghe, A. M. P. Tang and T. Brown, *Tetrahedron*, 2007, **63**, 3483–3490.
44 C. Beyer and H.-A. Wagenknecht, *Chem. Commun.*, 2010, **46**, 2230.
45 N. J. Greco and Y. Tor, *J. Am. Chem. Soc.*, 2005, **127**, 10784–10785.
46 W. H. Melhuish, *J. Phys. Chem.*, 1961, **65**, 229–235.
47 S. M. Ormson, R. G. Brown, F. Vollmer and W. Rettig, *J. Photochem. Photobiol., A*, 1994, **81**, 65–72.
48 R. W. Sinkeldam, N. J. Greco and Y. Tor, *Chem. Rev.*, 2010, **110**, 2579–2619.
49 L. Â. M. Wilhelmsson, *Quart. Rev. Biophys.*, 2010, **43**, 159–183.
50 M. Egli, N. Usman and A. Rich, *Biochemistry*, 1993, **32**, 3221–3237.
51 P. Auffinger and E. Westhof, *Angew. Chem. Int. Ed.*, 2001, **40**, 4648–4650.
52 M. Vorlíčková, I. Kejnovská, K. Bednářová, D. Renčiuk and J. Kypr, *Chirality*, 2012, **24**, 691–698.
53 W. Saenger, W. N. Hunter and O. Kennard, *Nature*, 1986, **324**, 385–388.
54 W. Saenger, *Principles of Nucleic Acid Structure*, Springer-Verlag, New-York, 1984.
55 A. P. Demchenko, *J. Mol. Struct.*, 2014, **1077**, 51–67.